ChemComm

COMMUNICATION

View Article Online
View Journal | View Issue

Cite this: *Chem. Commun.*, 2016, 52, 7564

Received 26th April 2016,
Accepted 11th May 2016

DOI: 10.1039/c6cc03502g

www.rsc.org/chemcomm

Influence of nucleobase stoichiometry on the self-assembly of ABC triblock copolymers†

Keren Zhang,[a] Samantha J. Talley,[a] Ya Peng Yu,[b] Robert B. Moore,[a] Mitsuhiro Murayama[b] and Timothy E. Long*[a]

ABC triblock copolymers bearing adenine- and thymine-functionalized external blocks self-assembled into long-range, ordered lamellar microphase-separated morphologies on non-patterned substrates. Intermolecular hydrogen bonding formed thymine–adenine triplets and promoted self-assembly into well-defined lamellae consisting of poly(*n*-butyl acrylate) soft domains and complementary nucleobase hard domains, while thymine–adenine duplets contributed to superior mechanical properties.

Immiscibility of chemically different segments of block copolymers drives their self-assembly behavior, which generates various microphase-separated morphologies with periodic arrays of domains ranging from 10 to 100 nm in size.[1–3] Directed self-assembly of block copolymer thin films on patterned substrates forms well-defined periodic arrays of nano-size features with designed shapes, and the subsequent selective removal of one block enables fabrication of templates and scaffolds used in the microelectronics industry.[2,4,5] Advances in polymer synthesis expand the applications of functional block copolymers to drug delivery, material templates, nanoporous membranes, photonic materials, composite materials, solar cells, adhesives, and elastomers.[6–14]

Combining noncovalent interactions with microphase-separation of block copolymers potentially provides a synergistic influence on self-assembly behavior and enables precise nanoscale features with additional functionality. For example, Bazzi *et al.* synthesized the first self-complementary ABC triblock copolymers and observed sequence-dependent self-assembly behavior in solution.[15] Xiong *et al.* demonstrated the formation of long worm-like aggregates in solution from two diblock copolymers bearing hydrogen bonding donors and acceptors, respectively.[16] In the solid state, binary blends of two hydrogen-bonded diblock copolymers self-assembled into a highly asymmetric lamellar morphology.[17] Another study showed that blends of two diblock copolymers with short associating blocks self-assembled into various hierarchical nanophase-separated morphologies with varying blending ratios and film-casting conditions.[18]

ABC triblock copolymers generally self-assemble into complex morphologies with three phases in the solid state.[19–23] Our group recently synthesized ABC triblock copolymers with two complementary, nucleobase-functionalized external blocks and a poly(*n*-butyl acrylate) (poly(*n*BA)) central block.[24] Distinctive SAXS profiles revealed a highly ordered lamellar microphase-separated morphology of annealed ABC triblock copolymer films. However, the key parameters for achieving this ordered lamellar morphology remain undetermined. This manuscript studies the effect of block length and thymine–adenine (T–A) binding ratio on the morphology and thermomechanical properties to establish the structure–property–morphology relationship for ABC triblock copolymers with associating blocks. This study reveals synergistic effects of noncovalent interactions and microphase-separation on self-assembly and thermomechanical performance of block copolymers.

A prerequisite three-step RAFT polymerization afforded ABC block copolymers poly(thymine acrylate-*b*-*n*-butyl acrylate-*b*-adenine acrylate), abbreviated as poly(ThA-*b*-*n*BA-*b*-AdA) and PTBA (Fig. 1a and Table S1, ESI†), following earlier procedures of Long *et al.*[24] PTBA triblock copolymers were solution cast from DMSO into non-patterned PTFE molds and upon solvent vaporization, formed free-standing films ranging from 0.2 mm to 0.5 mm in thickness.

Varying poly(AdA) block length and maintaining poly(ThA) and poly(*n*BA) block lengths yielded a series of PTBA copolymer films with different microphase-separated morphologies. Fig. 1c summarizes the compositions, thymine–adenine molar ratios (T–A ratios), and nucleobase block weight percentages (NB wt%), as well as the morphologies of solution-cast PTBA films determined using SAXS and AFM. PTBA triblocks self-assembled into two phases (Fig. 1b), consistent with previous results.[24] Adenine- and thymine-functionalized blocks formed complementary hydrogen bonding

[a] *Department of Chemistry, Macromolecules Innovation Institute, Virginia Tech, Blacksburg, VA 24061, USA. E-mail: telong@vt.edu*
[b] *Department of Materials Science and Engineering, Virginia Tech, Blacksburg, VA, USA*

† Electronic supplementary information (ESI) available: Full experimental procedures and additional characterization data. See DOI: 10.1039/c6cc03502g

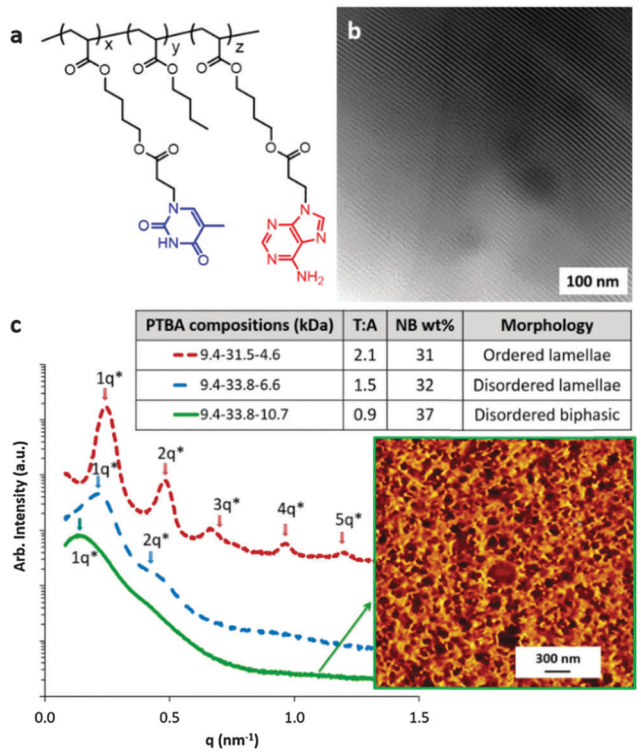

Fig. 1 (a) Chemical structure of poly(ThA-*b*-*n*BA-*b*-AdA) (PTBA) ABC triblock copolymers. (b) TEM image of the PTBA (9.4–31.5–4.6) triblock copolymer film. (c) SAXS profiles of PTBA films with varying thymine–adenine molar ratio; AFM phase image shows the disordered biphasic surface morphology of a PTBA (9.4–33.8–10.7) triblock copolymer film.

and assembled into an iodine-stained hard phase with T_g near 70 °C, and poly(*n*BA) internal blocks formed a soft phase with T_g near −45 °C (Fig. S2, ESI†).

Increasing the adenine-functionalized block length from 4.6 kDa to 10.7 kDa resulted in a decrease of the thymine–adenine molar ratio from 2.1 to 0.9. A distinctive scattering pattern for PTBA with a T–A molar ratio of 2.1 showed a well-organized lamellar morphology, while a T–A molar ratio of 1.5 led to a scattering profile with broader scattering peaks and only one distinguishable secondary peak at the 2*q* position, indicative of a disordered lamellar morphology. SAXS analysis of PTBA with a T–A molar ratio of 0.9 indicated a significantly less ordered morphology, and AFM showed a disordered biphasic morphology at the film surface. We previously proposed two hypotheses to account for different morphologies of PTBA copolymers with various compositions, *i.e.*, (1) the order of microphase-separated morphology increased with increasing block length, (2) the thymine–adenine molar ratio dominated self-assembly and affected the order of microphase-separation.[24] Since copolymers in Fig. 1 all exhibited similar long block lengths, it is reasonable to conclude that sufficient block length alone does not necessarily lead to a well-ordered morphology.

The thymine–adenine molar ratio likely plays a significant role in PTBA self-assembly. The order of the PTBA morphology increased as the T–A molar ratio changed from 1 : 1 to 2 : 1. Primary scattering peak positions corresponded to the domain spacings of lamellae. Increasing adenine block length from 4.6 kDa to 6.6 kDa to 10.7 kDa resulted in a significant increase of the domain spacing from 25.9 nm to 29.2 nm to 44.8 nm. AFM phase images showed the absence of the lamellar morphology on the film surface due to different surface energies of the nucleobase and poly(*n*BA) domains in air. However, the transmission electronic microscopy (TEM) image of the microtomed PTBA (9.4–31.5–4.6) film revealed a remarkably ordered lamellar morphology with long-range order (Fig. 1b and Fig. S3, ESI†). This long-range order likely resulted from complementary hydrogen bonding directing the assembly of the nucleobase blocks in the absence of a substrate pattern.

Dynamic mechanical analysis (DMA) displayed a different trend of thermomechanical performance (Fig. 2) from morphologies for the three PTBA copolymers films. The PTBA film with a T–A molar ratio near one exhibited the highest plateau modulus and the widest plateau regime with the least ordered morphology. 1 : 1 hydrogen bonding between thymine and adenine contributed to superior thermomechanical properties compared to 2 : 1 binding. Hydrogen bonding between adenine and thymine provided physical crosslinking in the hard phase, which restricted molecular mobility beyond the glass transition temperature[24] of the nucleobase block near 60–70 °C, observed only using DSC. A 1 : 1 binding ratio likely afforded stronger association strengths and more physical crosslinking than the 2 : 1 binding ratio. Moreover, increasing the nucleobase content from 31 wt% to 37 wt% provided another explanation for increased plateau modulus. Verification of these two hypotheses requires additional PTBA triblock copolymer films with different compositions.

An additional aspect of this investigation pertains to the morphological and thermomechanical differences for PTBA copolymers with a similar nucleobase wt% but different T–A molar ratios. Fig. 3 depicts two PTBA copolymers with a similar nucleobase weight percentages and different T–A molar ratios. The SAXS profile for PTBA (9.4–27.2–5.3) with a T–A molar ratio of 1.8 exhibited higher order scattering peaks up to the 5*q* position, indicative of an ordered lamellar morphology. On the contrary, PTBA (9.4–39.3–11.6) with a T–A molar ratio of 0.8 displayed significantly broader scattering peaks, indicative

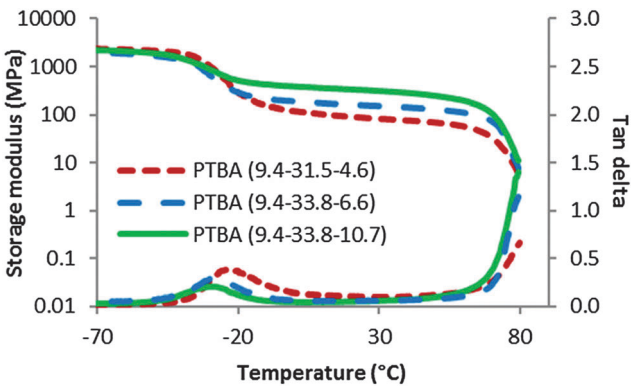

Fig. 2 Dynamic mechanical temperature ramps for solution-cast PTBA films with varying poly(AdA) block length.

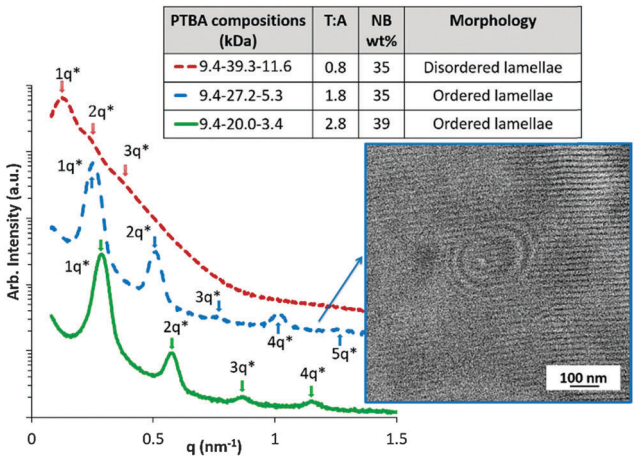

Fig. 3 SAXS profiles of PTBA films with varying thymine–adenine ratio or varying nucleobase block weight percent; TEM image shows ordered lamellar morphology of a PTBA (9.4–20.0–3.4) triblock copolymer film. *Newton's rings are imaging artifacts due to weak phase contrast.

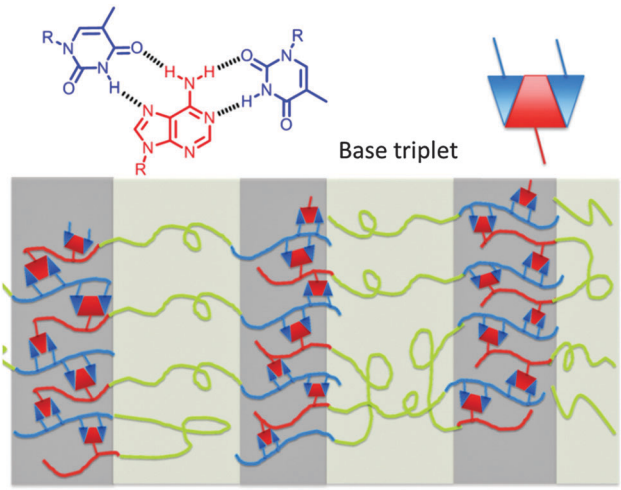

Fig. 4 Proposed pictorial representation of long-range ordered lamellar morphology of PTBA triblock copolymers that contain thymine–adenine base triplets.

of a disordered lamellar morphology, despite a similar nucleobase wt% to PTBA (9.4–27.2–5.3). This morphological difference indicated a strong dependence of the PTBA morphology on the thymine–adenine binding ratio, which yielded an ordered lamellar phase when the T–A molar ratio approached 2 : 1. The domain spacing of lamellae in Fig. 3 significantly increased with increasing block lengths, as the primary scattering peak shifted to lower q values.

A steric effect provides a plausible explanation for the optimal T–A binding ratio in achieving ordered lamellar morphology. The conjugated purine ring of adenine occupies a larger space than the pyrimidine ring of thymine. Two thymine units bind with one adenine unit to form a base triplet (Fig. 4), previously observed in triple helix DNA molecules.[25] PTBA (9.4–27.2–5.3) with a T–A ratio of 2.8 also self-assembled into ordered lamellae with scattering peaks up to the 4q position. Additional thymine units with a higher T–A ratio than 2 : 1 presumably caused less disruption to the triplet formation compared to additional adenine units. As a result, PTBA with T–A of 2.8 showed more ordered lamellae compared to PTBA with T–A of 0.8. The formation of base triplets likely facilitates the development of highly ordered lamellar morphology. However, the current study only places the optimal T–A ratio near 2 : 1, and determining the precise optimal ratio for forming lamellae with long-range order could be achieved with complementary computational simulations and calculations. The weight percentage of the overall nucleobase blocks showed an insignificant effect on self-assembled morphologies of PTBA for the entire series synthesized in this study (Table S1, ESI†).

Two symmetric ABA triblock copolymers carrying random copolymers ThA and AdA as external blocks served as controls to investigate the necessity of the asymmetric ABC triblock structure in forming an ordered lamellar morphology (Scheme S1, ESI†). SAXS and AFM results of ABA control with T–A of 1.9 showed a mixed cylindrical-lamellar morphology, distinctively different from the ordered lamellar morphology of PTBA (9.4–31.5–4.6) with a similar T–A molar ratio and nucleobase wt% (Fig. S4, ESI†). An ABA control with a T–A molar ratio of 1 : 1 showed a cylindrical morphology, also different from the disordered lamellar morphology of PTBA (9.4–39.3–11.6) with a similar T–A molar ratio and nucleobase wt%. Randomly distributed thymine and adenine predominately associated with their adjacent partners from the same block, resulting in typical morphologies of non-associating ABA triblock copolymers. The blends of two ABA triblock copolymers with thymine and adenine external blocks, respectively, also self-assembled into cylindrical morphologies.[26] The asymmetric ABC block copolymer structure facilitated the intermolecular recognition between adenine and thymine units from different polymer chains, which proved to be crucial for ordered lamellae formation.

Intermolecular hydrogen bonding presumably directed the packing of complementary nucleobase blocks, which assembled into the hard domains (Fig. 4). Well-organized lamellae with long-range order formed with an optimal space filling thymine–adenine molar ratio near 2 : 1 (Fig. 1b), while deviation of the T–A molar ratio resulted in disordering in the long-range stacking of the lamellae (Fig. S5, ESI†). Hydrogen bonding within the nucleobase-containing hard domains directed the morphological development of long-range ordered lamellae, and each nucleobase block preferentially bonded with its complementary block rather than the poly(nBA) block.

In contrast to the effect of T–A molar ratio on morphological ordering, thermomechanical profiles of PTBA copolymer films followed a strikingly different trend with varying T–A molar ratios. As shown in Fig. 5, PTBA1 with a T–A molar ratio of 0.8 exhibited a higher plateau modulus compared to PTBA2 with a T–A molar ratio of 1.8 and a similar nucleobase wt%. The plateau modulus further decreased for PTBA3 (9.4–20.0–3.4) as the T–A molar ratio increased to 2.8. This variation of plateau moduli confirmed the hypothesis that hydrogen bonding of thymine–adenine diminished as the T–A molar ratio deviated from 1.0, resulting in less physical crosslinking and thus a lower plateau modulus. Furthermore, PTBA4 (9.4–19.3–6.8) with a significantly lower molecular weight exhibited a similar plateau

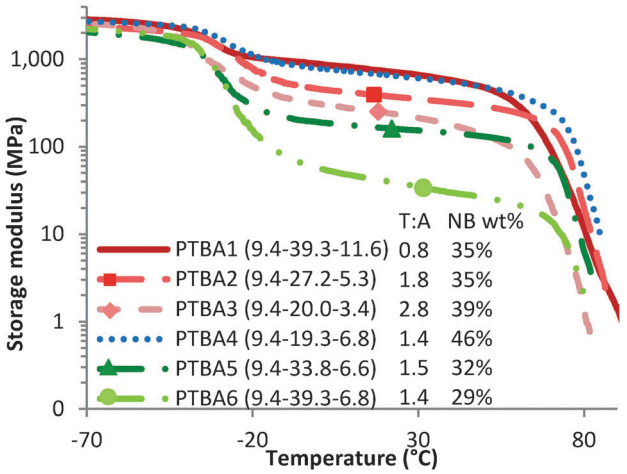

Fig. 5 Dynamic mechanical temperature ramps for solution-cast PTBA films with varying poly(*n*BA) and poly(AdA) block length.

modulus with PTBA1 (9.4–39.3–11.6), which suggested that the plateau modulus trend of PTBA1 > PTBA2 > PTBA3 did not result from their molecular weight difference.

Comparisons among PTBA4 through PTBA6 demonstrated that plateau modulus increased significantly with increasing nucleobase wt% at a constant T–A molar ratio. Higher nucleobase content resulted in a higher physical crosslinking density, thus improving the plateau moduli of the triblock copolymer films. Overall, the plateau moduli of PTBA copolymers increased with increasing nucleobase wt% and decreasing T–A molar ratio to 1.0. ^{1}H NMR titration experiments using the Job's method confirmed that the 1 : 1 host–guest binding stoichiometry was preferable for the complex of thymine acrylate and adenine acrylate in $CDCl_3$ (Fig. S6 and S7, ESI†).[27,28] A 1 : 1 binding ratio between thymine and adenine was favored thermodynamically, forming a stronger hydrogen-bonded network than the 2 : 1 base triplet.

In conclusion, ABC triblock copolymers with complementary, associating external blocks exhibited unique composition-dependent, self-assembled morphologies. Both the thymine–adenine molar ratio and nucleobase block weight percent influenced the bulk morphology and thermomechanical performance of solution-cast poly(ThA-*b*-*n*BA-*b*-AdA) copolymer films. An optimal thymine–adenine molar ratio near 2 : 1 promoted the formation of a long-range ordered lamellar morphology without substrate patterning. In contrast, thymine–adenine thermodynamically favored a 1 : 1 binding ratio, which provided the highest physical crosslink density and thus contributed to superior thermomechanical properties. The asymmetric structure of ABC triblock copolymers proved crucial in forming intermolecular hydrogen bonding, which directed the self-assembly into ordered lamellar phases. This study demonstrates the profound effect of noncovalent interaction on self-assembled morphology and thermomechanical performance of block copolymers. Utilizing the synergy of noncovalent interaction and block copolymer phase-separation provides a promising route for generating templates and scaffolds for nano-fabrication, as well as developing thermoplastics and elastomers with enhanced mechanical performance.

This work was supported in part by Henkel Corporation. This material was also partially based on work supported by the National Science Foundation under Grant No. DMR-0923107 and DMR-1507245.

Notes and references

1 F. S. Bates and G. H. Fredrickson, *Annu. Rev. Phys. Chem.*, 1990, **41**, 525.
2 C. M. Bates, M. J. Maher, D. W. Janes, C. J. Ellison and C. G. Willson, *Macromolecules*, 2014, **47**, 2.
3 K. Koo, H. Ahn, S.-W. Kim, D. Y. Ryu and T. P. Russell, *Soft Matter*, 2013, **9**, 9059.
4 H.-C. Kim, S.-M. Park and W. D. Hinsberg, *Chem. Rev.*, 2010, **110**, 146.
5 D. J. C. Herr, *J. Mater. Res.*, 2011, **26**, 122.
6 S. Förster and M. Antonietti, *Adv. Mater.*, 1998, **10**, 195.
7 P. Alexandridis and B. Lindman, *Amphiphilic block copolymers: self-assembly and applications*, Elsevier, 2000.
8 H. A. Klok and S. Lecommandoux, *Adv. Mater.*, 2001, **13**, 1217.
9 A. Rösler, G. W. Vandermeulen and H.-A. Klok, *Adv. Drug Delivery Rev.*, 2012, **64**, 270.
10 F. H. Schacher, P. A. Rupar and I. Manners, *Angew. Chem., Int. Ed.*, 2012, **51**, 7898.
11 K.-V. Peinemann, V. Abetz and P. F. W. Simon, *Nat. Mater.*, 2007, **6**, 992.
12 I. Botiz and S. B. Darling, *Mater. Today*, 2010, **13**, 42.
13 M. C. Orilall and U. Wiesner, *Chem. Soc. Rev.*, 2011, **40**, 520.
14 J. K. Kim, S. Y. Yang, Y. Lee and Y. Kim, *Prog. Polym. Sci.*, 2010, **35**, 1325.
15 H. S. Bazzi, J. Bouffard and H. F. Sleiman, *Macromolecules*, 2003, **36**, 7899.
16 D. a. Xiong, L. Shi, X. Jiang, Y. An, X. Chen and J. Lü, *Macromol. Rapid Commun.*, 2007, **28**, 194.
17 S. H. Han, V. Pryamitsyn, D. Bae, J. Kwak, V. Ganesan and J. K. Kim, *ACS Nano*, 2012, **6**, 7966.
18 K. Dobrosielska, A. Takano and Y. Matsushita, *Macromolecules*, 2010, **43**, 1101.
19 H. Nakazawa and T. Ohta, *Macromolecules*, 1993, **26**, 5503.
20 T. Higuchi, H. Sugimori, X. Jiang, S. Hong, K. Matsunaga, T. Kaneko, V. Abetz, A. Takahara and H. Jinnai, *Macromolecules*, 2013, **46**, 6991.
21 R. Stadler, C. Auschra, J. Beckmann, U. Krappe, I. Voight-Martin and L. Leibler, *Macromolecules*, 1995, **28**, 3080.
22 H. Elbs, C. Drummer, V. Abetz and G. Krausch, *Macromolecules*, 2002, **35**, 5570.
23 Y. Mogi, H. Kotsuji, Y. Kaneko, K. Mori, Y. Matsushita and I. Noda, *Macromolecules*, 1992, **25**, 5408.
24 K. Zhang, G. B. Fahs, M. Aiba, R. B. Moore and T. E. Long, *Chem. Commun.*, 2014, **50**, 9145.
25 S. Sivakova and S. J. Rowan, *Chem. Soc. Rev.*, 2005, **34**, 9.
26 K. Zhang, M. Aiba, G. B. Fahs, A. G. Hudson, W. D. Chiang, R. B. Moore, M. Ueda and T. E. Long, *Polym. Chem.*, 2015, **6**, 2434.
27 L. Fielding, *Tetrahedron*, 2000, **56**, 6151.
28 M. Tamami, S. T. Hemp, K. Zhang, M. Zhang, R. B. Moore and T. E. Long, *Polymer*, 2013, **54**, 1588.